Available online at www.sciencedirect.com
SCIENCE DIRECT®
Journal of Contaminant Hydrology 78 (2005) 343–371
JOURNAL OF Contaminant Hydrology
www.elsevier.com/locate/jconhyd

Numerical simulations of pyrite oxidation and acid mine drainage in unsaturated waste rock piles

J.W. Molson [a,*], O. Fala [a], M. Aubertin [a,c], B. Bussière [b,c]

[a] *Department of Civil, Geological and Mining Engineering, École Polytechnique de Montréal, P.O. Box 6079, Stn. Centre-ville, Montréal, Québec, Canada H3C 3A7*
[b] *Department of Applied Sciences, Université du Québec en Abitibi-Témiscamingue, 445 University Blvd., Rouyn-Noranda, Québec, Canada J9X 5E4*
[c] *NSERC Polytechnique/UQAT Chair, Environment and Mine Waste Management, Canada*

Received 16 August 2004; received in revised form 9 May 2005; accepted 3 June 2005

Abstract

Numerical simulations of layered, sulphide-bearing unsaturated waste rock piles are presented to illustrate the effect of coupled processes on the generation of acid mine drainage (AMD). The conceptual 2D systems were simulated using the HYDRUS model for flow and the POLYMIN model for reactive transport. The simulations generated low-pH AMD which was buffered by sequential mineral dissolution and precipitation. Sulphide oxidation rates throughout the pile varied by about two orders of magnitude (0.004–0.4 kg m^{-3} $year^{-1}$) due to small changes in moisture content and grain size. In the fine-grained layers, the high reactive surface area induced high oxidation rates, even though capillary forces kept the local moisture content relatively high. In waste rock piles with horizontal layers, most of the acidity discharged through vertical preferential flow channels while with inclined fine grained layers, capillary diversion channeled the AMD to the outer slope boundary, keeping the pile interior relatively dry. The simulation approach will be useful for helping evaluate design strategies for controlling AMD from waste rock.

Keywords: Waste rock piles; Acid mine drainage; Unsaturated flow; Sulphide oxidation; Reactive transport modelling

* Corresponding author. Tel.: +1 514 340 4711x5189; fax: +1 514 340 4477.
E-mail address: john.molson@polymtl.ca (J.W. Molson).

0169-7722/$ - see front matter © 2005 Elsevier B.V. All rights reserved.
doi:10.1016/j.jconhyd.2005.06.005

1. Introduction

Sulphide mineral oxidation within unsaturated waste rock piles can be the source of significant groundwater and surface water contamination. The effluent, commonly known as acid mine drainage (AMD), is generally characterized by low pH and high concentrations of sulphate, iron and dissolved metals (Jambor, 1994; Sracek et al., 2004). Much research is currently focused on defining the governing processes and designing methods for prevention and remediation of AMD (Johnson et al., 2000; Hurst et al., 2002; Schneider et al., 2002).

Often, the rate-limiting process for sulphide oxidation is the availability of sulphides within the waste rock particles, and the availability of oxygen at the mineral grain surfaces. Oxygen can be transported from the pile surface deep into the pile interior through diffusion in the gas phase, and by thermal or wind-induced convective transport (Lefebvre et al., 2001b; Ritchie, 2003; Kim and Benson, 2004). Within highly stratified or less permeable piles, diffusive transport may dominate and oxygen transport will be controlled by the moisture-dependent bulk diffusion rates. As the diffusion rate of oxygen in water is several orders of magnitude less than in air (Fredlund and Rahardjo, 1993; Collin and Rasmuson, 1988), the rate of oxygen diffusion will vary throughout the pile depending on the local water content (Mbonimpa et al., 2003).

Variations in the water content of a waste rock pile will also change its relative permeability and can create preferential flow paths for migration of the acidic effluent (Newman et al., 1997). Using numerical simulations of unsaturated flow, Fala (2002) and Fala et al. (2003, submitted for publication) show that small changes in water saturation can significantly affect the flow field within rock piles, causing preferential flow in higher saturation regions. They also show that fine-grained layers inclined downward toward the outer pile boundary can channel flow away from the interior through a process known as capillary diversion (as simulated, for example, by Oldenburg and Pruess, 1993). Fine grained layers can also act as moisture-retention barriers to oxygen diffusion, whereas coarser layers can be dryer and can allow rapid oxygen penetration (Bussière et al., 2003a,b).

The distribution of water within a waste rock pile will depend primarily on its internal structure and grain size distribution, which are becoming better understood through data collection and site characterization. Lefebvre et al. (2001a), for example, compared the physicochemical properties of waste rock piles in Quebec (Doyon) and Germany (Nordhalde). They found significant differences in physical and chemical properties and developed different conceptual models to explain the observed fluid and gas flow behaviour. Helgen et al. (2000) used measured profiles of oxygen, temperature and geochemistry to help interpret oxidation rates within various waste rock dumps in Nevada. They presented evidence supporting diffusive and convective-controlled oxygen gas transport. Further site characterization data are provided by Ritchie (1994a), Smith et al. (1995), Tran et al. (2003), and Price (2003).

In addition to the flow field and oxygen availability, other factors which govern sulphide oxidation rates include the fraction of sulphide minerals within the host rock, and the reactive surface area of the minerals. With sufficient oxygen, reaction rates will generally increase as the sulphide fraction and reactive surface area per volume of waste rock increases. Janzen et al. (2003), for example, found that particle surface area had a

major influence on oxidation rates of pyrrhotite, with higher rates in finer-grained material. In unsaturated waste rock piles, however, the dependence of oxidation rates on particle size can be more complex because fine-grained material may also retain more moisture which will typically reduce the availability of oxygen and decrease the oxidation rate. The interactions of these coupled and non-linear processes are not always intuitive and often require advanced flow and reactive transport models to help understand and predict their behaviour.

A variety of advanced numerical simulation tools have been developed over the past decade for simulating the governing processes of multi-component reactive mass transport and acid mine drainage in waste rock. A review of recent advances in AMD modelling is provided by Mayer et al. (2003).

Eriksson and Destouni (1997) applied a Langangian transport model to simulate flow and acid mine drainage. Their simulations included the coupled processes of kinetic (rate limited) mineral dissolution, secondary mineral precipitation and preferential flow on copper leaching from waste rock. Flow heterogeneities were represented with uni- and bi-modal probabilistic distributions. Their simulations showed that in systems with preferential flow, peak AMD loads were reduced but dispersed over longer time scales.

Nicholson et al. (2003) applied the 1D PHREEQC geochemical model to simulate transport and chemical reactions occurring in a waste rock pile at a uranium mine. Their conceptual model assumed that the oxidation rate was low enough that oxygen replenishment by diffusion could provide a non-limiting supply. Sulphide oxidation could therefore be described by oxygen-independent first-order kinetics. AMD loading rates were presented for current conditions at the mine, as well as for two cover scenarios. Similarly, Schneider et al. (2002) applied the PHREEQC model to the Schüsselgrund waste rock dump near Königstein, Germany. Their results were used to evaluate the feasibility of using reactive barriers for immobilizing uranium, zinc and radium.

Lefebvre et al. (2001b), and Sracek et al. (2004) present simulations of waste rock piles using the TOUGH/AMD code (based on the TOUGH2 model by Pruess, 1991) which considered air and water flow, pyrite oxidation, and transport of heat and sulphate. Their simulations were based on extensive site characterization data and showed the influence of convective gas flow due to oxidation-induced thermal gradients. Reaction rates were pre-assigned in their model while aqueous geochemical reactions and mineral precipitation and dissolution (e.g. pH buffering by carbonate or hydroxide minerals) were not considered. Linklater et al. (2005) applied the SULFIDOX 2D finite difference code to simulate sulphide mineral oxidation and AMD at the Aitik waste rock dump in Sweden. Their approach considered equilibrium and kinetic chemical reactions as well as heat generation and secondary mineral formation. Their flow system was considered steady state and their three conceptual models were homogeneous, each with a fixed bulk oxidation rate derived from field observations of oxygen consumption. They concluded that the reactive surface area of the sulphide minerals and selection of secondary minerals were significant sources of uncertainty.

Mayer et al. (2002) present an advanced model (MIN3P), which solves the fully-coupled problem of unsaturated flow and reactive mass transport using the locally mass-conservative finite volume method with a general kinetic and global implicit formulation. The model can consider gas, aqueous and solid phases, as well as surface and transport-

controlled reactions including the shrinking core model for sulphide oxidation. Bain et al. (2001) applied MIN3P to simulate the geochemical evolution of mine waters, including pH buffering and mineral dissolution/precipitation. MIN3P could not be used for the current study because it employs orthogonal brick elements and therefore cannot easily handle the sloping geometry required for the conceptual rock piles considered here.

Walter et al. (1994a) developed a 2D reactive transport model (MINTRAN) by coupling a finite element transport model for advective–dispersive mass transport with the MINTEQA2 model (Allison et al., 1991) for simulating equilibrium geochemical reactions. Later, Wunderly et al. (1996) added a 1D kinetic sulphide oxidation module which has since been applied by Bain et al. (2000) to simulate acid mine drainage from the Nickel Rim tailings site, and by Romano et al. (2003) to simulate oxygen diffusion barriers for mine tailings. Gerke et al. (1998) further modified the MINTRAN model to include 2D oxygen diffusion, sulphide oxidation and unsaturated flow. They applied the model to simulate acidic drainage from heterogeneous, unsaturated overburden piles at lignite mining sites in Germany.

The purpose of this paper is to investigate the impact of internal structure on the generation and evolution of acid mine drainage within conceptual waste rock piles. The study is completed using the POLYMIN finite element model (Molson et al., 2004) which incorporates oxygen diffusion, kinetic (diffusion-limited) sulphide oxidation, multi-component advective–dispersive transport, aqueous speciation, and mineral precipitation and dissolution. POLYMIN is derived from the MINTRAN model (as applied by Gerke et al., 1998) which has been modified here to include triangular elements and to use unsaturated flow fields and material properties from the HYDRUS model (Simunek et al., 1999). This paper builds upon the conceptual flow systems simulated by Fala et al. (submitted for publication), for 2D vertical cross-sections of structured waste rock piles.

The simulations are used to gain insight into how AMD is affected by system parameters including moisture content distribution, pile structure, oxygen concentrations and host rock mineralogy. The kinetic oxidation and geochemical speciation approach is unique for simulating structured waste rock piles since the sulfide oxidation rate is not fixed a priori, but is a natural outcome of the model, based on local physical properties and component concentrations. A base case system is first presented in Section 4 followed by a sensitivity analysis in Section 5. Although the model parameters are based on field data wherever possible, the simulations are conceptual and are not intended to be indicative of a specific field site.

2. Conceptual model of the waste rock pile

The conceptual model used in this study is based on a vertical 2D Cartesian cross-section of an unsaturated waste rock pile 100 m wide and 20 m high (Fig. 1). To justify the 2D approach, its transverse length is assumed much longer than its width. The centerline is assumed to be a symmetry divide, therefore only the right half-section is considered. The top and inclined external surfaces are exposed to atmospheric concentrations of oxygen and to precipitation and evaporation; water can drain freely from the bottom. Specific parameters for the base case model are provided in Section 4.

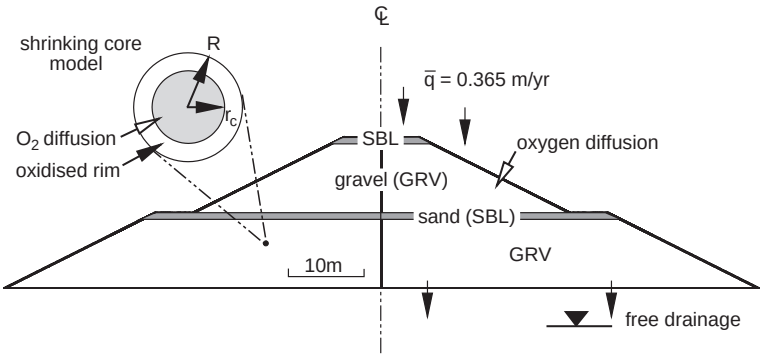

Fig. 1. Conceptual model developed for flow and transport simulations of waste rock piles. The simulations consider only the right-side symmetric 2D Cartesian section.

In this paper, the waste pile system is assumed composed of two homogeneous materials: two sand-size layers (SBL) within a host gravel (GRV) (Fig. 1). This conceptual model was adopted here (and by Fala et al., submitted for publication) in order to focus specifically on capillary barrier effects, due to different textural layers, on the generation of AMD. Additional macro-scale heterogeneities would not add significantly more insight in this context since (a) their properties and distribution are not yet well known for waste rock piles (but work is underway in the authors' group to investigate this aspect), and (b) the onset of preferential flow is controlled primarily by pore-scale material variability which cannot be simulated with conventional numerical methods at the scale of a waste rock pile. As will be shown in Section 4, we will take advantage of inherent flow system sensitivity to reproduce preferential flow systems in simple layered structures.

The two internal fine-grained layers within the model represent either natural compaction from depositional practices, or pre-designed features for controlling internal flow (Lamontagne et al., 2000; Lefebvre et al., 2001b; Aubertin et al., 2002; Fala et al., 2003; Wilson et al., 2003). A modified conceptual model is presented later in which the sand layers are inclined downward toward the external pile surface to induce flow diversion away from the interior.

The conceptual model assumes the following conditions: (1) the flow system is at steady state, (2) the pore water has a uniform density and temperature (10 °C), (3) pyrite oxidation is governed by the kinetic shrinking core model with spherical grains, (4) the geochemical speciation reactions are fast (equilibrium-controlled) relative to the flow field, (5) porosity and permeability are not affected by pile consolidation, or by mineral precipitation or dissolution, (6) evaporation does not affect the geochemistry, (7) gas transport is diffusion dominated, and (8) the rock pile is rapidly deposited relative to the bulk oxidation rate of the pile. In reality, the flow field and ambient temperatures are seasonally variable, sulphide oxidation is exothermic (which can lead to convective oxygen transport), and a waste rock pile may take years or even decades to build during which time the internal oxidized state may vary considerably due to pile growth. Furthermore, pH-buffering by silicate minerals (which can be kinetically-limited) has been replaced by a generic gibbsite and silica buffer. Sulphide oxidation rates are also assumed to be independent of microbial reactions under oxygen-limiting conditions (Ritchie, 1994b).

The above limitations are considered acceptable for the present study as the objective is to gain insight into the relative sensitivity of AMD to various system parameters. The assumption of steady state flow is perhaps most restrictive since transient events have been observed to significantly change the internal moisture distribution (Smith and Beckie, 2003; Fala et al., 2003). On the other hand, Linklater et al. (2005) also assumed steady flow, and found their predicted concentrations were consistent with observed long-term (>3 years) average data. In this paper, we take the latter approach and assume that the effect of seasonal flow variations on reactive transport will average out over the 20-year simulation time considered here. For more detailed calibration to specific sites, the transport model can easily incorporate a fully transient flow field.

The conceptual model for the reactive geochemical system is based on equilibrium speciation and pH-buffering by mineral precipitation/dissolution (Morin et al., 1988; Blowes et al., 1991). In the current study, the model includes reactive transport of 12 aqueous components (Ca, Mg, Na, K, Cl, CO_3, SO_4, Mn, Fe(II), Fe(III), H_4SiO_4 and Al), together with six existing or potential minerals (calcite, siderite, gibbsite, ferrihydrite, gypsum and amorphous silica) and oxygen. Except for the rate-limited oxidation of pyrite, all reactions are assumed equilibrium controlled. Although precipitation and dissolution of some minerals (e.g. silicates) may occur relatively slowly and violate the equilibrium assumption, this is not considered a significant limitation in this conceptual study.

Jurjovec et al. (2002) developed a similar geochemical conceptual model based on laboratory column experiments in which fresh unoxidized tailings were flushed with a sulphuric acid solution. Their observations support the concept of sequential buffering by carbonate minerals (ankerite–dolomite, siderite), as well as by gibbsite and aluminosilicates. Metal mobility was shown to be dependent on the pH of the effluent water. Although ferrihydrite was not present in their material, previous cases of pH buffering by secondary ferrihydrite have been observed (Blowes and Ptacek, 1994).

3. Numerical simulation approach

The numerical simulation approach for the waste rock piles was developed to be consistent with the conceptual model defined above. The simulations were completed by combining the HYDRUS/2D groundwater flow model (Simunek et al., 1999) with the reactive transport model POLYMIN (Molson et al., 2004). The models are coupled through the velocity field and moisture content distribution and use identical finite element grids based on linear triangular elements.

3.1. Unsaturated flow

The HYDRUS model solves the governing equation for Darcy-type fluid flow in a variably-saturated porous medium (Richards' equation), which can be written as:

$$\frac{\partial \theta_w}{\partial t} = \frac{\partial}{\partial x_i}\left[K_{ij}(\psi)\left(\frac{\partial \psi}{\partial x_j} + \frac{\partial z}{\partial x_j}\right)\right] - S \tag{1}$$

where θ_w is the (volumetric) water content (L^3L^{-3}), ψ is the pressure head [L], S is a sink term [T^{-1}], x_i ($i=1, 2$) are the spatial 2D Cartesian coordinates [L], t is time [T], and $K_{ij}(\psi)$ are the directional components of the unsaturated hydraulic conductivity function [LT^{-1}].

The water retention curves in the numerical simulations are represented by the van Genuchten (1980) relationship:

$$\theta_e = \frac{\theta_w - \theta_r}{\theta_s - \theta_r} = \left[\frac{1}{1+(\alpha\psi)^n}\right]^m \tag{2a}$$

and the hydraulic conductivity functions were estimated using the closed form analytical solution of the Mualem (1976) model proposed by van Genuchten (1980):

$$K(\theta_e) = K_s\theta_e^{\ell}\left[1-\left(1-\theta_e^{1/m}\right)^m\right]^2. \tag{2b}$$

In Eqs. (2a) and (2b), θ_e is the effective water saturation (L^3L^{-3}), θ_s is the saturated water content (or porosity), θ_r the residual water content, α, m, n are the van Genuchten (1980) parameters ($m=1-1/n$), $K(\theta_e)$ is the saturation-dependent hydraulic conductivity (LT^{-1}), K_s is the saturated hydraulic conductivity (LT^{-1}) and ℓ is a parameter representing the degree of pore connectivity ($\ell=0.5$ is used here, see Table 2).

The pressure head solution from Eq. (1) is used to derive the Darcy flux components q_i (LT^{-1}) for use in the transport model. The components are calculated according to:

$$q_i = -K_{ij}(\nabla\psi + \nabla z). \tag{3}$$

The local moisture contents (θ_w) are also passed to the transport model. Further information on the flow model and governing parameters are provided by Fala (2002).

3.2. Mass transport

Mass transport of the dissolved aqueous species (excluding O_2) is governed by the advection–dispersion equation with a reaction source/sink term. The transport equation in POLYMIN for aqueous component k ($k=1,\ldots,N_c$, where N_c is the number of components) is of the form:

$$\frac{\partial\theta_w C_k}{\partial t} = \frac{\partial}{\partial x_i}\left(\theta_w D_{ij}\frac{\partial C_k}{\partial x_j}\right) - \frac{\partial}{\partial x_i}(q_i C_k) + R_k \tag{4}$$

where C_k is the total aqueous concentration of the k^{th} component in the pore water [ML^{-3}], q_i is the i^{th} component of the volumetric water flux [LT^{-1}], D_{ij} is the dispersion tensor [L^2T^{-1}], and R_k is the source/sink term for the k^{th} component resulting from heterogeneous equilibrium reactions [$ML^{-3}T^{-1}$]. The components of the dispersion tensor, D_{ij}, are given by:

$$\theta_w D_{ij} = \alpha_T|q|\delta_{ij} + (\alpha_L - \alpha_T)\frac{q_i q_j}{|q|} + \theta_w D_d\tau\delta_{ij} \tag{5}$$

where D_d is the molecular diffusion coefficient in water [L^2T^{-1}], $|q|$ is the absolute value of the Darcy fluid flux [LT^{-1}], δ_{ij} is the Kronecker delta function, α_L and α_T are the

Table 1
Summary of major system variables for the numerical simulations, base case scenario

Parameter	Value
Porosity (θ)	0.39 (GRV gravel) 0.29 (SBL sand)
Water content (θ_w)	0.001–0.35[a]
Grain size D_{50} (mm)	5.0 mm (GRV) 0.5 mm (SBL)
Initial unoxidized fraction of grain radius (r_c/R)	0.9[b]
Henry's constant (H; $[O_2]_{air}/[O_2]_{water}$)	33.2
Temperature	10.0 °C
Bulk density (ρ_b)	1836 kg m^{-3}
Initial O_2 concentration	0.0003 g L_{air}^{-1}[b]
Oxygen diffusion coefficient through the bulk waste rock pile (D_e)	0.002–140 m^2 $year^{-1}$[a]
Oxygen diffusion coefficient through mineral grains (D_2)	10^{-6} m^2 $year^{-1}$[c]
Surface recharge (q)	0.365 m $year^{-1}$
Sulfide mineral fraction (f_s)	
SBL	0.001 $kg_{sulphur}$ kg_{solid}^{-1}
GRV	0.06 $kg_{sulphur}$ kg_{solid}^{-1}
Dispersivities (α_L, α_T)	0.5 m, 0.05 m[d]
Diffusion coefficient of dissolved chemical species in water (D_d)	0.005 m^2 $year^{-1}$

All values, except where noted, were obtained from measured or published data.
[a] Water content is determined by the flow solution and controls D_e (see Fig. 4 and Eq. (7)). D_e is based on an oxygen diffusion coefficient in air of $D_a = 1.8 \times 10^{-5}$ m^2/s, and that in water of $D_w = 2.1 \times 10^{-9}$ m^2/s; (Fredlund and Rahardjo, 1993).
[b] Assumed as initial condition (10% of radius pre-oxidized).
[c] From Romano et al. (2003), and Wunderly et al. (1996) who used 1×10^{-7}–3×10^{-7} m^2/year for tailings; and Gerke et al. (1998) who used 10^{-3} m^2/year for waste overburden.
[d] Based on system scale; see, for example, Gerke et al. (1998).

longitudinal and transverse vertical dispersivities, respectively [L], and $\tau = \theta_w^{7/3}\theta_s^{-2}$ is a tortuosity factor selected from Millington and Quirk (1961).

3.3. Oxygen diffusion

In the POLYMIN model, the air phase is assumed immobile (convection is neglected) and oxygen transport through the unsaturated rock waste is governed by the 2D equation for oxygen diffusion in a porous medium, expressed as:

$$\theta_{eq}\frac{\partial [O_2]_a}{\partial t} = D_e\left(\frac{\partial^2 [O_2]_a}{\partial x^2} + \frac{\partial^2 [O_2]_a}{\partial z^2}\right) - Q_{O_2} \quad (6)$$

where $[O_2]_a$ is the oxygen concentration in the air phase [ML^{-3}], θ_{eq} is the equivalent (water phase corrected) volumetric air content [L^3L^{-3}], D_e is the effective oxygen diffusion coefficient within the bulk unsaturated spoil [L^2T^{-1}], and Q_{O2} is the sink term for oxygen consumption due to sulphide mineral oxidation ($M_{O2}L^{-3}T^{-1}$) which depends on the diffusion rate through the waste particles (see Eq. (11)).

The equivalent air content θ_{eq} in Eq. (6) is defined here as $\theta_{eq} = \theta_a + \theta_w/H$ where θ_a is the air-filled porosity and H is Henry's Law coefficient for equilibrium oxygen partitioning

between air and water ($[O_2]_{air}/[O_2]_{water}$; see Table 1) (Aubertin et al., 1999, 2000). The oxygen diffusion coefficient D_e is represented in this study by the Aachib et al. (2002) model:

$$D_e = \frac{1}{\theta_s^2}\left[D_a\theta_a^{p_a} + \frac{D_w}{H}\theta_w^{p_w}\right] \tag{7}$$

where D_a and D_w are the diffusion coefficients in air and water, respectively, and p_a and p_w are fitting coefficients; here $p_a=p_w=3.3$ is assumed, as suggested by Aachib et al. (2002). Various other oxygen diffusion models, including those of Millington and Quirk (1961) or Elberling et al. (1993) can also be used; however for the generally low-saturation conceptual models used in this study, they gave almost identical responses for AMD prediction.

3.4. Sulphide oxidation

Within waste rock piles, the generation of acid mine drainage is controlled by the oxidation of sulphide minerals. The oxidation of pyrite by oxygen, for example, can be described in simplified form by the following stoichiometric equations (Stumm and Morgan, 1981):

$$FeS_2 + H_2O + 7/2O_2 \Rightarrow Fe^{2+} + 2SO_4^{2-} + 2H^+ \tag{8}$$

$$Fe^{2+} + 1/4O_2 + H^+ \Rightarrow Fe^{3+} + 1/2H_2O \tag{9}$$

$$FeS_2 + 1/2H_2O + 15/4O_2 \Rightarrow Fe^{3+} + 2SO_4^{2-} + H^+ \tag{10}$$

where oxidation proceeds either by Eq. (8), or depending on how much Fe^{2+} is oxidized to Fe^{3+}, by both Eqs. (8) and (9), which are equivalent to Eq. (10).

The rate of these oxidation reactions is controlled by the availability of oxygen at the surface of, and within the oxidized rim of the sulphide-containing grains. These reactions are simulated here using the well-known shrinking core model (Levenspiel, 1972) which assumes that the sulphide minerals are uniformly distributed within spherical grains of the host rock, and that the oxidation is rapid relative to oxygen diffusion within the grains. Derivations for this model have been presented by Davis and Ritchie (1986, 1987), Nicholson et al. (1990) and Gerke et al. (1998), and are not repeated here.

The rate of oxygen consumption Q_{O2} in Eq. (6) (equivalent to the intrinsic oxidation rate IOR, Ritchie, 2003) is defined by

$$Q_{O_2} = D_2\frac{3(1-\theta_s)}{R^2}\left(\frac{r_c}{R-r_c}\right)\frac{[O_2]_a}{H} \tag{11}$$

where D_2 is the effective diffusion coefficient [L^2T^{-1}] which incorporates the characteristic diffusion properties of the water film and the oxidized shell of the sulphide-bearing rock particle, R is the average radius of the particle [L], r_c is the average radius of the unreacted particle core [L], and $[O_2]_a$ is the oxygen concentration in the air phase in contact with the particle. Thus, the availability of oxygen at the sulphide mineral surface depends on both the bulk effective diffusion rate (D_e) through the air and water phases of the rock waste, as well as the diffusion rate through the mineral grains (D_2).

The decrease in the unoxidized core radius is determined using

$$\frac{dr_c}{dt} = \frac{D_w(1-\theta)}{\varepsilon \cdot \rho_s} \frac{R}{r_c(R-r_c)} \frac{[O_2]_a}{H} \tag{12}$$

where ε [−] is the mass ratio of oxygen to sulphur consumed on the basis of the reaction stoichiometry (see Eqs. (8) (9) (10)), and $\rho_s = f_s \cdot \rho_b$ where f_s (M_{Su}/M_{solids}) is the mass fraction of the sulphide mineral within each particle and ρ_b (ML^{-3}) is the bulk density. Using Eq. (12), and assuming equilibrium between Fe^{2+} and total Fe, the mass of each oxidation product generated can be determined for each oxidation time step Δt^{oxid} (Wunderly et al., 1996; Gerke et al., 1998).

In this approach, the sulphide oxidation rate is not fixed a priori, but is governed more naturally by the available oxygen at the grain surface, by the reactive surface area and by the fraction of sulphide minerals and oxygen diffusion rate within the solid grains. The reaction liberates SO_4^{2-}, Fe^{2+}, Fe^{3+} and H^+, which can then react with other aqueous components and background minerals, and be transported downgradient. This conceptual model is consistent with previous studies including those of Gerke et al. (1998) and Bain et al. (2001).

3.5. Solution strategy

POLYMIN uses the two-step sequential non-iterative approach (SNIA) to couple the physical and chemical domains. This method has been shown to provide efficient and accurate solutions for a variety of problems provided the time step Δt is sufficiently small (Valocchi and Malmstead, 1992; Walter et al., 1994a; Steefel and MacQuarrie, 1996). A small but acceptable time discretisation error originates from the operator split approach, as shown by Calderhead and Mayer (2004).

The simulation over a transport time step Δt begins with an iterative solution to the oxygen diffusion and reactive core equations which liberates H^+, SO_4^{2-}, Fe^{2+} and Fe^{3+}. Because of the nonlinearity of these coupled reactions, the diffusion/core reaction part is performed over a smaller sub-time step Δt^{oxid}, typically 1/10th–1/50th of the transport time step Δt. These calculations are very rapid and do not significantly affect the total execution time. The reactive products are accumulated and added to the existing nodal concentrations just before the chemical equilibration step which is completed independently by the MINTEQA2 module at each grid node. Full details on the numerical approach are provided in Molson et al. (2004).

The transport and chemical steps account respectively for about 1/3 and 2/3 of the total execution times. A typical 20-year, 15,000-node simulation using a P-IV, 2.0 Ghz machine required on the order of 48 h.

4. Simulated base case system

Working with the conceptual model described in Section 2, a base case (Scenario 1) is first defined and the simulation results shown in detail. In Section 5, a sensitivity analysis is provided in which various system parameters that can potentially affect acid mine

drainage are changed. All simulations were run to a maximum of 20 years, by which time the rate of oxygen diffusion and AMD had reached a pseudo steady state condition.

4.1. Definition of the base case model

The base case system contains two sulphide-bearing solid materials: a relatively coarse grained gravel-type material (GRV) forming the bulk of the pile waste and a finer grained sand-size material (SBL), which forms two horizontal interior layers (Fig. 1; see also Fala et al., submitted for publication: Scenario S3). Each sand layer is 0.5 m thick and is continuous across the width of the pile. The lower layer extends from 9.5–10.0 m elevation, while the upper layer extends from 19.5 m to the pile surface at 20 m.

The right-half symmetric sections of each waste rock model were resolved using triangular element grids containing on the order of 14,000–18,000 nodes (Fig. 2), depending on the geometry of each scenario. Element dimensions range from about 5 cm within the two fine-grained SBL layers to 20 cm within the coarser gravel near the base of the pile. The Peclet accuracy constraint ($\Delta x_i < 2\alpha_L$) is satisfied by designing a sufficiently refined mesh, and the Courant stability constraint ($\Delta t < \Delta x_i / v_i$) is satisfied using a constant time step of 0.005 years (1.8 days).

The flow systems used here are based on the steady state, 5-year solution from the transient water seepage simulations of Fala et al. (submitted for publication). The precipitation and evapo-transpiration rates were based on observed data at the Latulipe mine site in northern Quebec (Fala et al., submitted for publication). In this paper, seasonal changes in the flow systems are assumed to have only secondary effects on the long-term behaviour of AMD. The lower flow boundary in each scenario is free-draining and assigned a fixed potential of −5.0 m, while the left boundary represents a no-flow symmetry divide.

The physical parameters of the waste rock (Table 1) are loosely based on observed data from the waste rock pile at Mine Doyon, Quebec (Gélinas et al., 1994; Poirier and Roy,

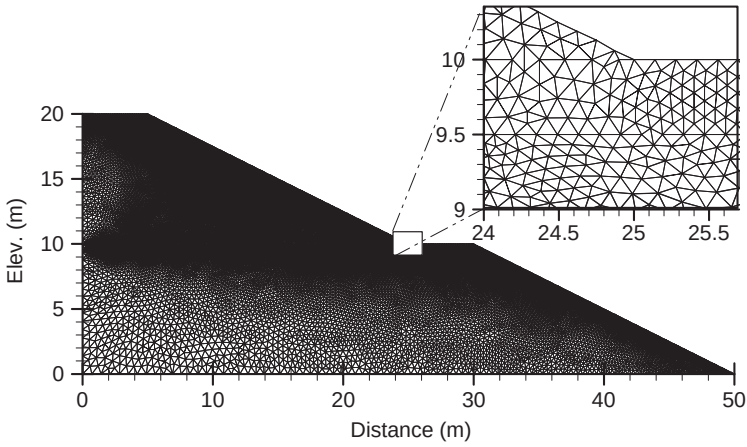

Fig. 2. A 2D finite element grid representing the waste rock pile; inset shows mesh detail for defining the lower sand layer.

Table 2
Values of the van Genuchten (1980) parameters used in the current study

	θ_r	θ_s	α (m)	ℓ	n	K_s (ms^{-1})
GRV	0	0.39	14,960	0.5	1.45	4.7×10^{-3}
SBL	0.01	0.29	3	0.5	3.72	5.1×10^{-5}

GRV=host waste rock, SBL=sand-size material.
Parameters based on measured data from Bussière (1999).

1997; Sracek et al., 2004). The Doyon waste rock pile is about 30 m high and is composed primarily of sericite schists and diorite with a pyrite mass fraction ranging from about 0.06–0.07 (6–7 wt.%). Although Sracek et al. (2004) found evidence for convective influx of oxygen at sites close to the pile slope, diffusive oxygen transport dominated toward the pile centre and at depth. The role of convective oxygen transport was also less significant during the recharge period compared to the dry period.

In most simulation scenarios presented here, the host waste rock (GRV) and finer sand-size layers (SBL) contain reactive sulphide minerals. In the base case, for example, the GRV material is assumed to contain 6 wt.% pyrite, while the finer SBL layers contain only 0.1 wt.% pyrite. This represents a condition where the sand material has been pre-processed, or has been obtained from a relatively sulphur-free source.

The van Genuchten (1980) parameters used to describe water retention in the sand and gravel are provided in Table 2 and the water retention curves and corresponding hydraulic conductivity functions are shown graphically in Fig. 3. Although the water retention curves used in the flow model are based on an observed, heterogeneous pore-size distribution, the transport model assumes average uniform grain sizes for the GRV and

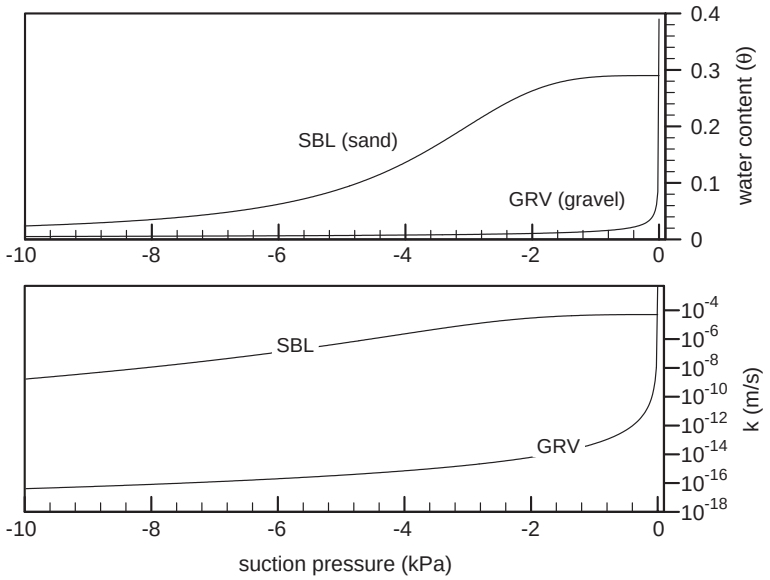

Fig. 3. Water content and hydraulic conductivity curves used in the model for the sand (SBL) and gravel (GRV) materials (see Table 2 for the van Genuchten parameters; after Fala et al., submitted for publication).

SBL material of 5.0 and 0.5 mm, respectively, consistent with grain sizes from the Laronde, Goldstrike and Doyon waste rock piles (Gamache-Rochette, 2003; Martin et al., 2004; Sracek et al., 2004; respectively).

The initial background mineralogy and chemical composition are also loosely based on data from the Doyon mine (Table 3). Observed minerals include calcite and various silicates including feldspar, muscovite and chlorite (Sracek et al., 2004). Principal secondary minerals are gypsum and K-jarosite. The mineralogy of the base case scenario is a simplified representation of the observed conditions, assuming some pre-oxidation prior to deposition (the shrinking-core model assumes an initially non-zero oxidized shell thickness; here we assume 10% pre-oxidation, see Table 1).

In the base case simulation, an initial background calcite concentration of 0.1 mol L^{-1} is assumed (following past conventions and using consistent MINTEQ units, solid concentrations are here expressed as moles per litre of water). Amorphous silica (used as a surrogate for the reactive silicate components), as well as gibbsite and gypsum (from pre-oxidation) are also initially present at 1.0 mol L^{-1}. Siderite and ferrihydrite are not present initially, but are allowed to precipitate as secondary pH-buffering minerals. Except for pyrite, all mineral components are assumed to be in thermodynamic equilibrium with the local aqueous composition.

Across the upper surface and sloping pile boundary, recharge with a chemical composition typical of rainwater is applied as a third-type (Cauchy) condition (Table 3). The lower discharge boundary is a second-type, zero-gradient (Neumann) condition,

Table 3
Inflow boundary and initial background concentrations for all components in the waste rock model

Component	Conc. (mol L^{-1})	
	Recharge water[a]	Equilibrated background
Ca	2.0 e–05	1.5 e–02
Mg	2.0 e–05	3.2 e–03
Na	7.0 e–05	1.1 e–03
K	5.0 e–06	5.1 e–04
Cl	2.0 e–05	5.0 e–04
CO_3	2.0 e–05	3.7 e–03
SO_4	7.4 e–05	1.7 e–02
Mn	1.0 e–06	3.0 e–04
Fe(II)	2.2 e–16	2.5 e–05
Fe(III)	1.0 e–08	2.1 e–08
H_4SiO_4	1.0 e–08	1.9 e–03
Al	1.0 e–10	3.0 e–08
pH	6.1	7.0
Calcite	n/a	0.10
Siderite	n/a	0.00
Gypsum	n/a	1.00
Ferrihydrite	n/a	1.0 e–04
Gibbsite	n/a	1.0
Am. Silica[b]	n/a	1.0

[a] Consistent with Mayer et al. (2002) and Appelo and Postma (1993).
[b] Amorphous silica.

allowing a natural outflow of all aqueous components. Oxygen is applied as a first-type boundary condition across all exposed surfaces (at an atmospheric concentration of 0.265 g/L_{air}) from where it diffuses into the pile interior. It equilibrates with the incoming recharge at the boundary and with local moisture within the pile.

4.2. Moisture distribution and water flow

The flow system for the base case transport model was taken from the 5-year solution of the HYDRUS model, as presented by Fala et al. (submitted for publication) (Flow Scenario S3: 2D Cartesian geometry, horizontal layers). The flow simulation is shown in Fig. 4a where streamtraces highlight preferential flow through the zones of higher moisture content. The two 0.5 m-thick finer grained sand-sized layers are clearly evident

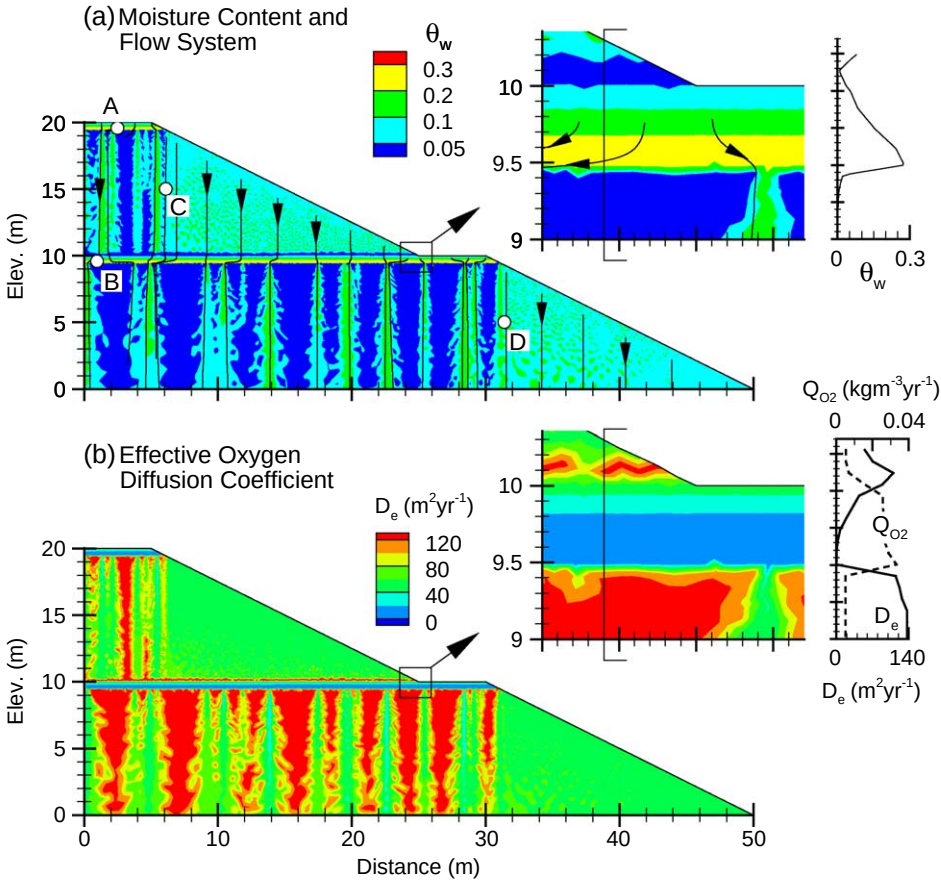

Fig. 4. Base case (Scenario 1) simulation showing (a) moisture content distribution (θ_w) and stream traces, and (b) effective oxygen diffusion coefficient (D_e). Enlarged views include vertical profiles of (a) moisture content and (b) D_e and Q_{O2} (oxidation rate at 20 years) across the lower sand layer. Letters refer to locations of arrival curves for Fig. 7.

as horizontal zones where the pores, at least toward the bottom of these layers, are nearly saturated (θ_w=0.29). These layers are behaving as capillary barriers (Bussière et al., 2003a,b), with moisture preferentially retained relative to the surrounding coarser grained waste rock (GRV). Below each layer, channels of higher-saturation form due to localized drainage from the sand layers. These channels occur approximately every 2–5 m along the sand layers, and appear where the local fluid pressure first reaches the water entry pressure of the coarser waste rock material.

In a real waste rock pile with similar layering, flow channels would occur naturally due to intrinsic heterogeneities in the materials and along the interface and also due to pore-scale variations in the moisture content. As the local moisture content within the SBL layer reaches the water entry pressure of the underlying GRV, the flow system becomes highly sensitive to small scale moisture perturbations which may then develop into a preferred flow channel (Oldenburg and Pruess, 1993; Newman et al., 1997). The numerical flow model reproduces these channels somewhat serendipitously from local grid orientation effects. Mass balance and convergence was verified for all flow simulations, and hydraulic conductivities back-calculated from the simulated water contents were verified to match those predicted from the van Genuchten input function (using the verification approach described by Chapuis et al., 2001). Since pore scale material variability cannot be simulated at the scale of a waste rock pile, even a heterogeneous conductivity or grain size distribution at the grid element scale would not reproduce the true physical mechanisms. Further details on the flow systems are provided by Fala et al. (submitted for publication).

Between the flow channels, the host waste rock remains relatively dry, and moisture contents are on the order of a few percent. Below the boundary flanks of the pile, the moisture content is again slightly higher due to natural infiltration.

4.3. Oxygen diffusion and pH

Oxygen diffusion through the pile is controlled by the effective (bulk) oxygen diffusion coefficient (D_e in Eq. (7)) which is inversely proportional to the local moisture content. In this base case simulation, the lowest diffusion coefficients appear at the base of the near-saturated sand layers (D_e=0.01–0.1 m^2 $year^{-1}$), and to a lesser extent within the preferential flow zones (D_e=30–60 m^2 $year^{-1}$) while the highest coefficients appear within the relatively dryer waste rock material (D_e=120–130 m^2 $year^{-1}$) (Fig. 4b).

As oxygen diffuses through the pile, it is consumed by oxidation of the pyrite fraction within the grains and the pH drops (Fig. 5). The simulation after 2 years shows that oxygen diffuses rapidly through the air space of the unsaturated pile with oxygen concentration contours generally following the pile surface boundaries. Consumption of oxygen occurs throughout the pile, but is particularly noticeable towards the top of the two fine-grained sand layers at 9.5 and 19.5 m elevations. Oxygen concentrations are significantly lower below these sandy layers compared to concentrations above. Oxygen influx is further slowed due to the higher moisture content at the base of the fine-grained sand which reduces the local effective diffusion coefficient.

The waste rock pile is relatively dry below the two sand layers which allows rapid oxygen diffusion, and the oxidation rates are sufficiently low that internal oxygen concentrations reach 20% of the atmospheric (boundary) concentration after 2 years

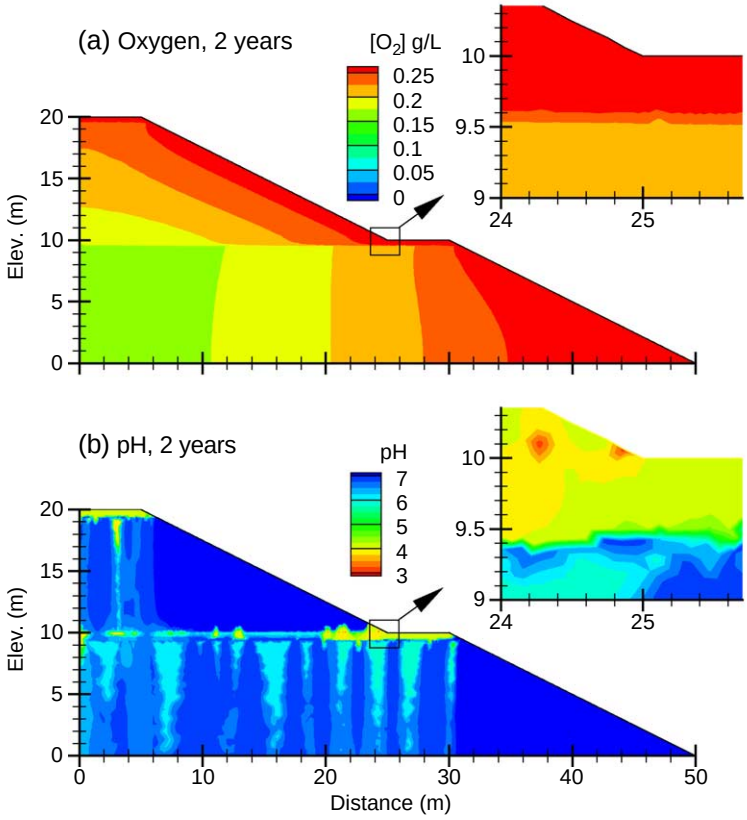

Fig. 5. Simulated oxygen concentrations and pH after 2 years, base case Scenario 1.

(Fig. 5a), and 100% after 5 years (not shown). The simulated behaviour is consistent with the conceptual model in which oxygen convection has been neglected. Under these conditions, convection-induced oxygen transport would not significantly affect the results.

After 2 years, the diffusion of oxygen and subsequent pyrite oxidation has reduced the pH in some parts of the pile to about 4 (Fig. 5b), and to about 3 after 20 years (Fig. 6). Several mechanisms are responsible for this pH distribution. First, low-pH zones develop within the relatively dry areas below the SBL layers (between the preferential flow zones) because oxygen is more readily available compared to the wetter areas, and because the fluid here is immobile and hence the oxidation products can accumulate. Secondly, the pH drops within the SBL layers (even though the sulphide fraction is lower than in the GRV) because of their finer grain size and hence larger reactive surface area per unit volume of waste rock relative to the coarser GRV. The lower moisture content in the upper part of the sandy layers relative to the bottom of these layers also facilitates oxygen diffusion and increases pyrite oxidation. However, the effect is limited since this lower moisture content is still higher than in the coarser GRV material.

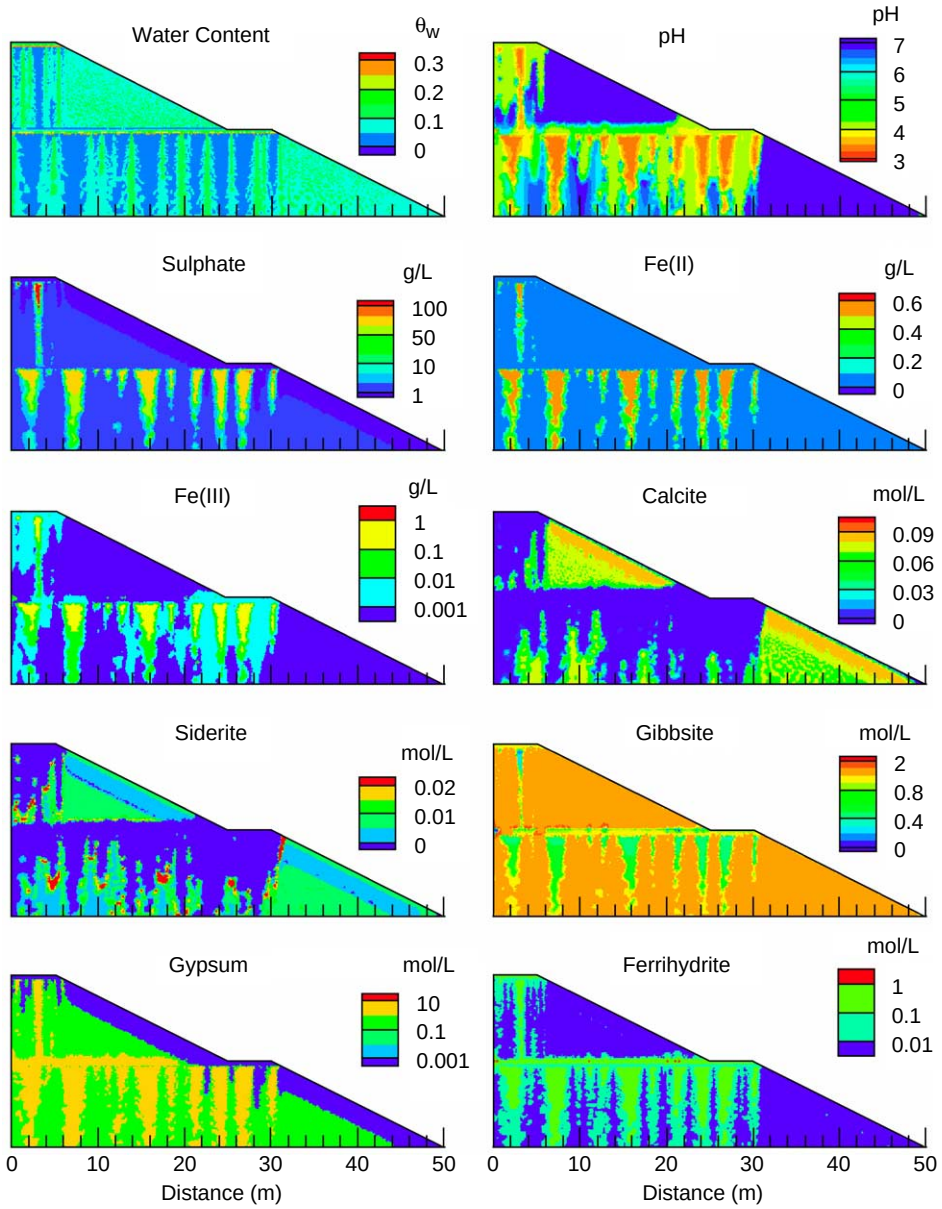

Fig. 6. POLYMIN simulation showing moisture content, pH and selected aqueous and solid mineral species after 20 years, base case Scenario 1.

The pH is also low within the vertical preferential flow zones of the host waste rock where the moisture content is relatively higher. These zones serve as preferential flow pathways which transport acidity and oxidation products from areas of high oxidation within the overlying sand layers. The pH here is thus controlled by the physical process of

advective–dispersive transport rather than by reactive geochemistry. The intrinsic oxidation rate within the preferential flow zones is actually quite low due to the coarse grain size which limits the reactive surface area, and due to the relatively higher moisture content which limits oxygen diffusion.

Thus it appears in this base case scenario that that the reactive surface area is the rate-limiting parameter for pyrite oxidation. Reduced oxygen diffusion due to higher water content appears to be of secondary importance for the conditions induced here. The simulations also suggest that low-pH zones can be found in relatively drier or wetter regions of an unsaturated waste rock pile. Under this conceptual model, low-pH regions may or may not be serious contributors to AMD as the environmental impact will also depend on the local flow rates through the pile.

Although we were not attempting to simulate a given site, the simulated pH range is consistent with that observed at the Doyon site for which Sracek et al. (2004) observed minimum pH levels on the order of 2–2.5, and with pH levels of 2.9–3.3 as observed for the Schüsselgrund waste rock dump (Schneider et al., 2002). A minimum pH of 3.3 was also reported at the Aitik waste rock site, Sweden, by Linklater et al. (2005).

4.4. Oxidation products and mineral buffering

In addition to lowering the pH, pyrite oxidation releases sulphate and iron as direct oxidation products, as well as any available metals mobilized by the lower pH (for example aluminum is released from gibbsite dissolution). These components react in the model with the existing minerals and aqueous components and are concurrently transported downwards through the pile.

The simulated concentrations for all major aqueous components and minerals for the base case Scenario 1, after 20 years, are provided in Fig. 6. The results show that even within a simple dual-media layered system, the generation of AMD is a complex function of the water content, oxygen concentration, grain size and background mineralogy.

In this base case scenario, aqueous sulphate concentrations reach about 100,000 mg L^{-1} and total iron concentrations reach over 1000 mgL^{-1}. These levels are again consistent with those at the Doyon site where Sracek et al. (2004) observed maximum sulphate concentrations (at Site 6) on the order of 100,000–200,000 mg L^{-1} and total iron ranging from 2000–20,000 mg L^{-1} (during the April recharge period, Site 6 at Doyon showed diffusive-controlled conditions). The behaviour of iron was somewhat difficult to interpret in the Mine Doyon study because of pH-dependent Fe(III) mineral precipitation (Sracek et al., 2004). In the current study, Fe(II) concentrations are generally higher than those for Fe(III), as above a pH of about 3, Fe(III) is precipitated as ferric hydroxide ($Fe(OH)_3$).

Simulated aluminum concentrations from gibbsite dissolution (not shown) reached a maximum of about 20,000 mg L^{-1} while observed values at Doyon Site 6 were on the order of 10,000 mg L^{-1} during the recharge period and 33,500 mg L^{-1} during the dry period. The highest simulated concentrations of aluminum appeared within the dryer immobile zones of the GRV where the oxidation products accumulate, and within the sand layers and vertical flow pathways connected to these layers.

It should be recognized that these high aqueous concentrations yield ionic strengths beyond the acceptable range for using Debye-Hückel and Davies-based activity coefficients (Ptacek and Blowes, 2003). However, under these conditions, the simulations can be considered conservative since the activity coefficients calculated by MINTEQA2 will be under-predicted and therefore the simulated aqueous concentrations will tend to be somewhat higher than those expected in the field. Furthermore, such high concentrations can cause density effects which are not considered here. Since the highest concentrations (e.g. sulphate) are found within the lower-saturation immobile zones, such density effects may be minimal.

Background minerals also play an important role in buffering the acidity generated through sulphide oxidation. In the conceptual geochemical model adopted here, calcite acts as the first pH-buffer, maintaining a pH of about 6.8 wherever calcite still exists. Because of its finite supply, calcite becomes completely dissolved from the low-pH regions after 20 years, and is significantly depleted in other areas. Siderite serves as the next pH-buffer, at a pH of about 5.2, precipitating where the carbonate concentration is high due to calcite dissolution, and where Fe(II) is high due to sulphide oxidation, i.e. around the margins of the advancing calcite dissolution zones. Gibbsite serves as the third pH-buffer at a pH of 3.8–4.2. Gibbsite dissolution releases aluminum (which originates from silicate mineral dissolution) and if additional metal hydroxides were present, they too could dissolve and release toxic metals as the low-pH front passes (see Walter et al., 1994b). Although not present initially, ferrihydrite precipitates where iron concentrations and pH levels are sufficiently high, and subsequent ferrihydrite dissolution can also buffer the pH when the low-pH front (pH 2.8–3.0) advances (Jurjovec et al., 2002; Johnson et al., 2000). Finally, gypsum precipitation is caused by calcite dissolution and elevated sulphate concentrations from pyrite oxidation.

4.5. Base case oxidation rates

Further insight into the reactive transport processes can be gained from the effective oxidation rate, as computed in the model from Q_{O2} in Eq. (6). This rate will vary throughout the pile and will change over time as oxygen concentrations change and as the unoxidized core radii (r_c) decrease. Within the upper sand layer, for example, the oxidation rate in this base case scenario initially increases as oxygen diffuses into the pile, then decreases over time because the reactive surface area of the grains is decreasing and oxygen has to diffuse farther through the oxidation rim. Within the SBL sand, the rate decreases from a maximum of about 0.40 kg(O_2) m^{-3} $year^{-1}$ (at 1 year) to 0.035 kg(O_2) m^{-3} $year^{-1}$ after a 20-year period (Fig. 7). Within the pile interior, which is characterized by the coarser grained waste rock material (GRV), the rates are 1–2 orders of magnitude lower. These simulated rates compare favourably with measured rates observed by Linklater et al. (2005) at the Aitik mine in Sweden (avg. = 0.32 kg(O_2) m^{-3} $year^{-1}$) and by Ritchie (2003; see his Notation Table), who cites a "typical" intrinsic oxidation rate of 0.3 kg(O_2) m^{-3} $year^{-1}$ (within a range of 0.015–150 kg(O_2) m^{-3} $year^{-1}$).

A mass balance analysis indicated that after 20 years, essentially all the pyrite within the SBL layers had been oxidized. However, this represented less than 1% of the initial

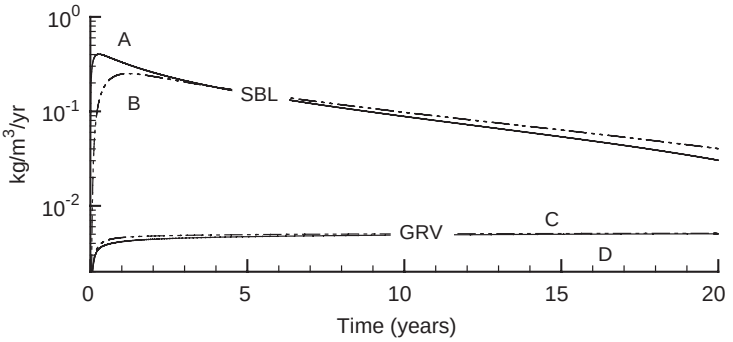

Fig. 7. Simulated sulfide oxidation rate vs. time at selected points within the pile, base case Scenario 1 (see Fig. 4 for point locations).

sulphide mass since the bulk of the sulphide exists within the coarser grained host material in which oxidation occurs much more slowly (Fig. 7).

5. Sensitivity analysis

Waste rock piles are naturally heterogeneous and variations in mineralogy, grain size and sulphur content can significantly affect oxidation rates and AMD. In this section, eight additional simulation scenarios are presented to gain insight into how a waste pile pH can be affected by the amount of sulphur, by variations in the diffusion coefficient through the grains, and by the calcite content (Table 4). Scenarios 2–6 have horizontal sand layers and are based on the same flow system as that used in the base case scenario. Scenarios 7, 8 and 9 have layers inclined 8° toward the outer pile boundary. The pH distribution after 20 years of oxidation is provided in Fig. 8 for all sensitivity scenarios listed in Table 4. The base case is repeated in Fig. 8 for ease of comparison.

In Scenario 2, the sulphur fraction of the sand layers is set to zero, leaving all other parameters identical to the corresponding base case Scenario 1. In this case, the

Table 4
List of simulation scenarios. Scenarios 1–6 have horizontal layers; scenarios 7–9 include sand layers which are inclined 8° toward the pile boundary

Scenario	Sulphur fraction (f_s)		D_2 (m^2 year^{-1})	Calcite (mol L^{-1})	Inclination angle (°)
	GRV	SBL			
1. Base case	0.06	0.001	10^{-6}	0.1	0
2. Sulphur-free SBL	0.06	0.000	10^{-6}	0.1	0
3. High sulphur SBL	0.06	0.06	10^{-6}	0.1	0
4. High D_2	0.06	0.001	10^{-5}	0.1	0
5. High calcite	0.06	0.001	10^{-6}	1.0	0
6. Low calcite	0.06	0.001	10^{-6}	0.0	0
7. Inclined SBL layers, base case	0.06	0.001	10^{-6}	0.1	8
8. Inclined SBL layers, sulphur-free SBL	0.06	0.000	10^{-6}	0.1	8
9. Inclined SBL layers, high sulphur SBL	0.06	0.06	10^{-6}	0.1	8

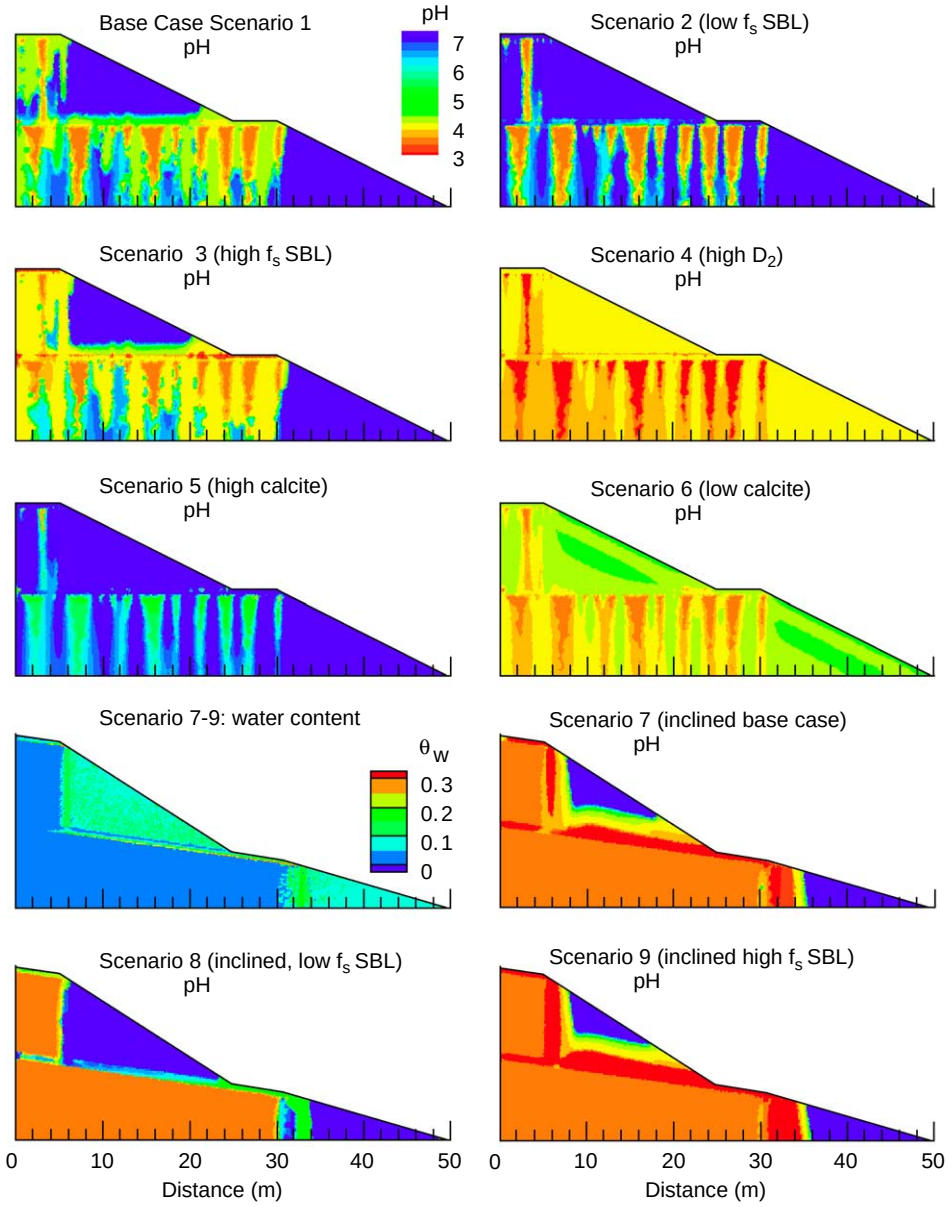

Fig. 8. Simulated pH distribution showing comparison between all scenarios after 20 years. Also shown is the water content for Scenarios 7–9 with inclined SBL layers.

preferential flow zones which previously carried low-pH effluent from the oxidizing sand are now more neutral, however in the dryer GRV between the preferential flow zones, the pH remains in the 3–4 range. Similar to the base case, oxidation continues in these drier

zones because of relatively higher oxygen diffusion rates. However, as flow rates are lower within these drier regions, this acidity again remains relatively immobile.

In Scenario 3, the sulphur content of the two sand layers is increased to the same fraction as that of the host gravel material (f_s=0.06). This would represent a case, for example, in which the sand layers were derived from the same material as the bulk waste rock. The results show a more extensive pH drop within the sand, reaching a minimum pH of about 3 along the entire length of each layer. In addition, this low-pH water has migrated further down along the preferential flow channels due to greater dissolution of calcite under these lower pH conditions.

In Scenario 4, the oxygen diffusion coefficient within the grains (D_2) of the host waste rock (GRV) and sand (SBL) is increased from 10^{-6} m^2 $year^{-1}$ in the base case to 10^{-5} m^2 $year^{-1}$. This would represent the case where the intra-grain porosity is higher, or where the grain mineralogy has been modified. The higher diffusion coefficient increases the oxidation rate throughout the pile, reduces the pH and increases the sulphate and iron concentrations. Although the minimum pH does not change significantly because of mineral buffering, the impact throughout the pile is significantly more extensive. In this scenario, calcite and siderite have completely dissolved throughout the waste pile and gibbsite dissolution has also increased relative to the base case (not shown).

In Scenario 5, the background calcite concentration is increased from 0.1 mol L^{-1} to 1.0 mol L^{-1}. As the increased mass of calcite provides a greater buffer capacity, the oxidation-induced pH-drop occurs later relative to the base case. However, the impact is limited as there is sufficient acidity to eventually dissolve all calcite within the preferential flow zones, after which the pH will be controlled by the remaining minerals. The higher calcite mass simply extends the time period over which the pH is calcite-buffered, and delays the pH drop to its siderite-buffered level. After 20 years, the minimum pH in the stagnant zones is about 5, while most of the host GRV is at about pH=6.8, buffered by the calcite. Siderite and gypsum concentrations are also higher in this case due to the longer time available for precipitation of these secondary minerals.

Scenario 6 assumes there is no calcite within the sand and waste rock material and the result after 20 years is a more uniform pH drop throughout the pile. The pH in the sand layers and preferential flow zones is essentially the same as in the base case (on the order of 3) as the pH is being controlled by the same calcite-free mineralogy – calcite having been completely dissolved in the base case, and not present initially in this scenario. Within the rest of the pile, however, particularly in the zones beneath the surface slopes, there is a significant pH drop relative to the base case. In the base case, sufficient calcite remains in these areas to buffer the pH, while in this scenario calcite is absent and the pH therefore drops quickly to levels similar to those found in the rest of the pile.

Scenario 7 is identical to the base case, however the fine-grained sand layers are now inclined at an angle of 8° downwards toward the outside pile surface to help channel flow away from the pile interior and towards the outer slope boundary. In this scenario, the preferred flow channels have disappeared since the pressure head has been reduced within the SBL units and thus the water entry value of the underlying GRV is not reached until the downslope limit of the layers. Most of the internal rock waste below the SBL layers therefore remains very dry (see moisture content plot for Scenario 7 in Fig. 8). These areas are therefore now characterized by more uniformly low-pH water which remains

effectively immobile because of the low flow rates. Although the minimum pH in this system has not changed significantly from the base case, the flux of acidity and oxidation by-products is essentially eliminated below most of the sand, and is instead focused near the downslope edge (see also Section 6, Fig. 10) where it can be more easily managed. Furthermore, if the pile flanks and SBL layers are constructed of low-sulphur material, this design could be used to help control production of AMD.

In Scenario 8, the sulphur mass fraction of the inclined sand is reduced from 0.001 to zero. The pH within the SBL layers is now near-neutral with only some minor pH decreases due to dispersion from the interface with the sulphide-containing GRV host. This simulation scenario produced the least amount of AMD within the waste rock piles considered here and highlights the advantage of constructing internal fine-grained layers using low reactive or sulphur-free material.

Finally, in Scenario 9, the sulphur fraction of the inclined sand is increased to 0.06, identical to that of the host GRV. The response is similar to the inclined base case (scenario 7), however the pH drop within the SBL is somewhat more extensive. The sand layers again become the dominant source of acidity but all acid mine discharge remains focused at the down-dip limit.

6. Comparison of pyrite oxidation and acid mine drainage

The response of the conceptualized waste rock pile to the imposed conditions for the various scenarios of Section 5 is compared in Fig. 9, showing the mass of sulphur oxidized, or released (as sulphate) from pyrite oxidation. Of all scenarios considered, Scenario 4 (horizontal SBL, high D_2) oxidized the most amount of sulphur over the 20-year. period while Scenario 8 (inclined SBL, low f_s) oxidized the least. The total mass of oxidized sulphur did not significantly depend on the inclination of the SBL layers (with other parameters constant), however the relative effect varied depending on the sulphur fraction within the layers (compare S1/S7, S3/S9, and S2/S8). Under high f_s conditions, for example, where most oxidation occurs within the SBL layers, sulphur in the inclined

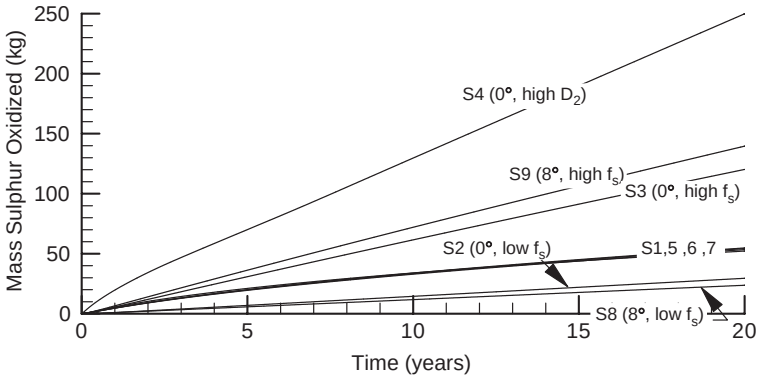

Fig. 9. Comparison over time of sulphur mass (per transverse metre of the pile) released from pyrite oxidation. Labels refer to simulation scenario (S1–9) and inclination angle of SBL layers (0–8°).

system (S9) tended to oxidize more rapidly relative to the equivalent horizontal case (S3). The reverse was observed for the low f_s (sulphur-free SBL) case in which all sulphur oxidation occurs within the GRV. Preferential flow and differences in water saturation therefore play important roles on the rate of sulphide oxidation. Changing the background concentration of calcite (Scenarios 5 and 6) had no effect on the oxidized sulphur mass since background buffer minerals do not affect the rate of pyrite oxidation, only the neutralizing capacity of the rock pile.

The net result of the reactive processes and transport within a waste rock pile is the discharge of acidity, sulphate and metals from the base of the pile, and possibly into groundwater or surface water. One measure of this environmental impact is the flux of AMD across the base of the pile. This discharge can be highly non-uniform due to the variable moisture content and preferential flow systems throughout the pile.

The simulated Darcy flux, water content, pH and sulphate flux across the base of the waste rock pile, for the two base case scenarios (horizontal and inclined SBL layers), are

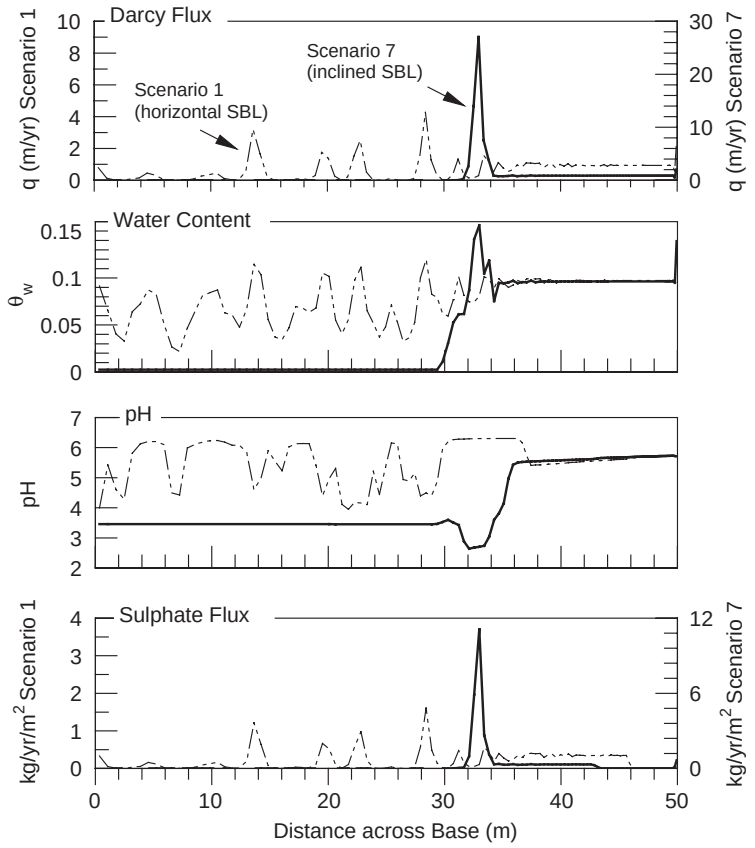

Fig. 10. Profiles across the bottom of the waste rock pile for Scenario 1 (horizontal SBL layers) and Scenario 7 (inclined SBL layers) showing Darcy flux, water content, pH and sulfate flux after 20 years. Note 3× scale increase for the Darcy flux and sulfate flux of Scenario 7.

provided in Fig. 10. The Darcy flux shows four prominent peaks which correspond to the preferential flow paths seen in Fig. 4. These high flow zones can be correlated with areas of higher moisture content and with low pH zones resulting from transport of acidified water from above. Similarly, the pH depressions correspond to peaks in the sulphate flux across the pile base. The net discharge of sulphate in this case varies on average from 0.0 to about 2.0 kg $year^{-1}$ m^{-2}.

With inclined layers, however, the sulphate flux has been eliminated across most of the pile base, but increases sharply in the preferential flow zone formed where the sand layer meets the pile slope at 30 m. Peak sulphate discharge for the inclined base case is 12 kg m^{-2} $year^{-1}$, respectively. Although this is about 6 times higher than in the corresponding horizontal base case, the flux is now more localized which may facilitate collection and control. Further simulations are underway to find optimal conditions to limit AMD and to assess the long-term oxidation behaviour.

7. Summary and conclusions

The behaviour of acidic mine drainage within unsaturated waste rock piles has been simulated using a multi-component pyrite oxidation and reactive transport model.

The base case simulation results were consistent with observed data at the Doyon mine, with minimum simulated pH levels of 2.8 and maximum sulphate and ferrous iron concentrations of 100,000 mg L^{-1} and 1000 mg L^{-1}, respectively. Oxidation rates predicted by the model varied from about 0.4 kg(O_2) m^{-3} $year^{-1}$ (after 1 year) to 0.035 kg(O_2) m^{-3} $year^{-1}$ after 20 years, and the maximum local sulphate flux across the pile base was approx. 2 kg m^{-2} $year^{-1}$ for the horizontal base case and 12 kg m^{-2} $year^{-1}$ for the inclined base case.

The waste rock pile conceptual models focused on the effects of moisture-retaining capillary barriers composed of finer, sand-sized material within a coarser gravel-sized host. Although these layers can limit oxygen diffusion, the simulations show that the increased reactive surface area of the finer grained material can render these layers significant sources of acidity and oxidation by-products. To limit AMD, capillary layers must therefore be designed using relatively non-reactive or sulphur-free material. If only sulphur-containing material is available, its grain size should be the maximum possible to limit the reactive surface area but the grains should remain small enough to retain sufficient moisture to maintain the preferential flow system. Using internal fine grained capillary barriers inclined at 8° towards the pile surface helped channel essentially all AMD into narrow discharge zones at the end of each sand layer, which may help facilitate AMD management. Further simulations and experiments are required to optimize these design parameters.

While the oxygen diffusion coefficient through the bulk waste rock is a critical factor, there was not a significant difference in the AMD simulations between several different conceptual models for the bulk oxygen diffusion coefficient. AMD was more significantly affected by the local diffusion coefficient through the porous grains (D_2), the determination of which should become a more important part of a site characterization program.

The AMD simulations presented here support the conclusions made by Sracek et al. (2004) who stress the importance of considering physical and geochemical processes together when predicting the behaviour and acid-generating potential of waste rock piles. To help determine the potential for AMD, it is necessary to understand the moisture distribution and flow system together with the grain size distribution, oxygen concentrations, geochemistry and pile mineralogy. For example, low-pH water which accumulates within stagnant flow zones will not contribute to AMD loading.

The simulations have provided more insight into the controlling processes and serve as a preliminary step to more advanced and site-specific geochemical transport modelling. The approach is being used to help design effective remediation strategies for existing waste rock piles and to develop new strategies of waste rock deposition and AMD control measures for proposed sites.

Acknowledgements

We thank Dr. Ondra Sracek (Masaryk University, Brno) for his helpful advice, as well as two anonymous reviewers for their constructive comments which significantly helped to improve this manuscript. This research was financially supported by the Natural Sciences and Engineering Research Council of Canada (NSERC) and by the partners of the Polytechnique-UQAT Industrial Chair in Environment and Mine Waste Management (www.polymtl.ca/enviro-geremi).

References

Aachib, M., Aubertin, M., Mbonimpa, M., 2002. Laboratory measurements and predictive equations for gas diffusion coefficient of unsaturated soils. Proceedings of the 55th Canadian Geotechnical and Joint IAH-CNC and CGS Groundwater Speciality Conference, Niagara Falls Ont. Canadian Geotechnical Society, Ottawa, pp. 163–171.

Allison, J.D., Brown, D.S., Novo-Gradac, K.J., 1991. MINTEQA2/PRODEFA2, a geochemical assessment model for environmental systems: version 3.0 user's manual. EPA/600/3-91/021, Environmental Research Laboratory, Office of Research and Development, U. S. Environmental Protection Agency, Athens, Georgia, U.S.A.

Appelo, C.A.J., Postma, D., 1993. Geochemistry, Groundwater and Pollution. A.A. Balkema, Rotterdam.

Aubertin, M., Bussière, B., Joanes, A.-M., Monzon, M., Gagnon, D., Barbera, J.-M., Bédard, C., Chapuis, R.P., Bernier, L., 1999. Projet sur les barrières sèches construites à partir de résidus miniers, Phase II: essais en place, Mine Environment Neutral Drainage (MEND) Report 2.22.2c, CANMET Secretariat, Ottawa, Ont.

Aubertin, M., Aachib, M., Authier, K., 2000. Evaluation of diffusive gas flux through covers with a GCL. Geotext. Geomembr. 18, 215–233.

Aubertin, M., Fala, O., Bussière, B., Martin, V., Campos, D., Gamache-Rochette, A., Chouteau, M., Chapuis, R.P., 2002. Analyse des écoulements de l'eau en conditions non-saturées dans les haldes à stérile, In Proceedings of: Symposium 2002 Rouyn-Noranda, Canadian Institute of Mining, Metallurgy and Petroleum, on CD-ROM.

Bain, J., Blowes, D.W., Robertson, W.D., Frind, E.O., 2000. Modelling of sulfide oxidation with reactive transport at a mine drainage site. J. Contam. Hydrol. 41 (1–2), 23–47.

Bain, J.G., Mayer, K.U., Blowes, D.W., Frind, E.O., Molson, J.W., Kahnt, R., Jenk, U., 2001. Modelling the closure-related geochemical evolution of groundwater at a former uranium mine. J. Contam. Hydrol. 52 (1–4), 109–135.

Blowes, D.W., Ptacek, C.J., 1994. Acid neutralization mechanisms in inactive mine tailings (Chapter 10). In: Blowes, D.W., Jambor, J.L. (Eds.), The Environmental Geochemistry of Sulfide Mine-Wastes, Short Course Handbook, vol. 22. Mineralogical Association of Canada, Waterloo, Ontario, pp. 271–292.

Blowes, D.W., Reardon, E.J., Jambor, J.L., Cherry, J.A., 1991. The formation and potential importance of cemented layers in inactive sulphide mine tailings. Geochim. Cosmochim. Acta 55, 965–978.

Bussière, B., 1999. Étude du comportement hydrique de couvertures avec effets de barrière capillaire inclinés à l'aide de modélisations physiques et numériques. PhD Thesis, Mineral Engineering Department, École Polytechnique de Montréal, Canada, 354 pp.

Bussière, B., Aubertin, M., Chapuis, R., 2003a. The behaviour of inclined covers used as oxygen barriers. Can. Geotech. J. 40 (3), 512–535.

Bussière, B., Apithy, S., Aubertin, 2003b. Diversion Capacity. CGC.

Calderhead, A.I., Mayer, K.U., 2004. Comparison of the suitability of the global implicit method and the sequential non-iterative approach for multicomponent reactive transport modelling. Proceedings of the 57th Canadian Geotechnical and 5th Joint IAH-CNC and CGS Groundwater Speciality Conference. Canadian Geotechnical Society, Quebec City, pp. 32–39.

Chapuis, R.P., Chenaf, D.C., Bussière, B., Aubertin, M., Crespo, R., 2001. A user's approach to assess numerical codes for saturated and unsaturated seepage conditions. Can. Geotech. J. 38 (5), 1113–1126.

Collin, M., Rasmuson, A., 1988. Gas diffusivity models for unsaturated porous media. Soil Sci. Soc. Am. J. 52, 1559–1565.

Davis, G.B., Ritchie, A.I.M., 1986. A model of oxidation in pyritic mine waste: Part 1. Equations and approximate solution. Appl. Math. Model 10, 314–322.

Davis, G.B., Ritchie, A.I.M., 1987. A model of oxidation in pyritic mine waste: Part 3. Importance of particle size distribution. Appl. Math. Model. 11, 417–422.

Elberling, B., Nicholson, R.V., David, D.J., 1993. Field evaluation of sulphide oxidation rates. Nord. Hydrol. 24, 323–338.

Eriksson, N., Destouni, G., 1997. Combined effects of dissolution kinetics, secondary mineral precipitation, and preferential flow on copper leaching from mining waste rock. Water Resour. Res. 33 (3), 471–483.

Fala, O., 2002. Étude des écoulements non saturés dans les haldes à stériles à l'aide de simulations numériques, Mémoire de maîtrise (M.Sc.A., unpublished), Génie Minéral, Dépt. CGM, École Polytechnique de Montréal, Canada.

Fala, O., Aubertin, M., Molson, J.W., Bussière, B., Wilson, G.W., Chapuis, R., Martin, V., 2003. Numerical modelling of unsaturated flow in uniform and heterogeneous waste rock piles. In: Farrell, T., Taylor, G. (Eds.), Sixth International Conference on Acid Rock Drainage (ICARD), Australasian Institute of Mining and Metallurgy, Cairns, Australia, Publication Series 3/2003, pp. 895–902.

Fala, O., Molson, J.W., Aubertin, M., Bussière, B., submitted for publication. Numerical modelling of flow and capillary barrier effects in unsaturated waste rock piles. Mine Water Environ.

Fredlund, D.G., Rahardjo, R., 1993. Soil Mechanics for Unsaturated Soils. John Wiley and Sons, Inc., New York.

Gamache-Rochette, A., 2003. Water flow characterization in unsaturated rock waste piles using in situ hydrogeological tests. MSc. Thesis (in French), Ecole Polytechnique, Montreal.

Gélinas, P., Lefebvre, R., Choquette, M., Isabel, D., Locat, J., Guay, R., 1994. Monitoring and modelling of acid mine drainage from waste rock dumps : Mine Doyon case study. Report GREGI 1994-12, Final Report Presented to MEND Prediction Committee, DSS contract 23440-3-9231/01-SQ, Natural Resources Canada.

Gerke, H.H., Molson, J.W., Frind, E.O., 1998. Modelling the effect of chemical heterogeneity on acidification and solute leaching in overburden mine spoils. Journal Hydrol. 209, 166–185 (Special issue: reactive transport modelling).

Helgen, S., Davis, A., Byrns, C., 2000. Measurement of oxygen, temperature and geochemical profiles in sulphide and oxide waste rock dumps of different ages. Proceedings, Fifth International Conference on Acid Rock Drainage. Society for Mining, Metallurgy and Exploration, Inc., Littleton, U.S.A.

Hurst, S., Schneider, P., Meinrath, G., 2002. Remediating 700 years of mining in saxony: a heritage from ore mining. Mine Water Environ. 21, 3–6.

Jambor, J.L., 1994. Mineralogy of sulfide-rich tailings and their oxidation products (Chapter 3). In: Jambor, J.L., Blowes, D.W. (Eds.), Short Course Handbook on Environmental Geochemistry of Sulfide Mine Wastes. Mineralogical Association of Canada, pp. 59–102.

Janzen, M.P., Nicholson, R.V., Scharer, J.M., 2003. The role of enhanced particle surface area, crystal structure and trace metal content on pyrrhotite oxidation rates in tailings. Proc Sudbury 2003: Mining and the Environment, CD-ROM, 1121 pp.

Johnson, R.H., Blowes, D.W., Robertson, W.D., Jambor, J.L., 2000. The hydrogeochemistry of the Nickel Rim mine tailings impoundment, Sudbury, Ontario. J. Contam. Hydrol. 41, 49–80.

Jurjovec, J., Ptacek, C., Blowes, D., 2002. Acid neutralization mechanisms and metal release in mine tailings: a laboratory column experiment. Geochim. Cosmochim. Acta 66 (9), 1511–1523.

Kim, H., Benson, C.H., 2004. Contributions of advective and diffusive oxygen transport through multilayer composite caps over mine waste. J. Contam. Hydrol. 71, 193–218.

Lamontagne, A., Fortin, S., Poulin, R., Tasse, N., Lefebvre, R., 2000. Layered co-mingling for the construction of waste rock piles as a method to mitigate acid mine drainage – laboratory investigations. Proceedings, 5th International Conference on Acid Rock Drainage (ICARD 2000), vol. 1. Society of Mining, Metallurgy and Exploration Inc., Denver Colorado, pp. 779–788.

Lefebvre, R., Hockley, D., Smolensky, J., Gélinas, P., 2001a. Multiphase transfer processes in waste rock piles producing acid mine drainage: 1. Conceptual model and system characterization. J. Contam. Hydrol. 52, 137–164.

Lefebvre, R., Hockley, D., Smolensky, J., Lamontagne, A., 2001b. Multiphase transfer processes in waste rock piles producing acid mine drainage: 2. Applications of numerical simulation. J. Contam. Hydrol. 52, 165–186.

Levenspiel, O., 1972. Chemical Reaction Engineering, 2nd ed. J. Wiley and Sons, New York.

Linklater, C.M., Sinclair, D.J., Brown, P.L., 2005. Coupled chemistry and transport modeling of sulphidic waste rock dumps at the Aitik mine site, Sweden. Appl. Geochem. 20, 275–293.

Martin, V., Aubertin, M., Bussière, B., Chapuis, P.R., 2004. Evaluation of unsaturated flow in mine waste rock. 57th Canadian Geotechnical Conference and the 5th joint CGS-IAH Conference, Canadian Geotechnical Society 24–27 October 2004, Quebec City.

Mayer, K.U., Frind, E.O., Blowes, D.W., 2002. Multicomponent reactive transport modeling in variably saturated porous media using a generalized formulation for kinetically controlled reactions. Water Resour. Res. 38 (9), 1–21 (13).

Mayer, K.U., Frind, E.O., Blowes, D.W., 2003. Advances in reactive-transport modelling of contaminant release and attenuation from mine-waste deposits (Chapter 14). In: Jambor, J.L., Blowes, D.W., Ritchie, A.I.M. (Eds.), Environmental Aspects of Mine Wastes, Short Course, vol. 31. Mineralogical Association of Canada, pp. 283–302.

Mbonimpa, M., Aubertin, M., Aachib, M., Bussière, B., 2003. Diffusion and consumption of oxygen in unsaturated cover materials. Can. Geotech. J. 40 (5), 916–932.

Millington, R.J., Quirk, J.M., 1961. Permeability of porous solids. Trans. Faraday Soc. 57, 1200–1207.

Molson, J.W., Frind, E.O., Aubertin, M., Blowes, D., 2004. POLYMIN: A Reactive Mass Transport and Sulphide Oxidation Model, User Guide. Ecole Polytechnique, Montreal.

Morin, K.A., Cherry, J.A., Dave, N.K., Lim, T.P., Vivyurka, A.J., 1988. Migration of acidic groundwater seepage from uranium-tailings impoundments: 1. Field study and conceptual hydrogeochemical model. J. Contam. Hydrol. 2, 271–303.

Mualem, Y., 1976. A new model for predicting the hydraulic conductivity of unsaturated porous media. Water Resour. Res. 12 (3), 513–522.

Newman, L.L., Herasymiuk, G.M., Barbour, S.L., Fredlund, D.G., Smith, T., 1997. The hydrogeology of waste rock dumps and a mechanism for unsaturated preferential flow. Proceedings of the 4th Int Conf on Acid Rock Drainage (ICARD), Vancouver, BC, vol. 2. Natural Resources Canada, Ottawa, pp. 551–564.

Nicholson, R.V., Gillham, R.W., Reardon, E.J., 1990. Pyrite oxidation in carbonate-buffered solution: 2. Rate control by oxide coatings. Geochim. Cosmochim. Acta 54, 395–402.

Nicholson, R.V., Rinker, M.J., Acott, G., Venhuis, M.A., 2003. Integration of field data and a geochemical transport model to assess mitigation strategies for an acid-generating mine rock pile at a uranium mine. Proceedings, Sudbury 2003: Mining and the Environment, CD-ROM.

Oldenburg, C., Pruess, K., 1993. On numerical modeling of capillary barriers. Water Resour. Res. 29 (4), 1045–1056.

Poirier, P., Roy, M., 1997. Acid mine drainage characterization and treatment at La Mine Doyon. Proc Fourth Int Conf on Acid Rock Drainage (ICARD), Vancouver, BC, vol. 4. Natural Resources Canada, Ottawa, pp. 1487–1497.

Price, W.A., 2003. The mitigation of acid rock drainage: four case studies from British Columbia. Proc Sudbury 2003: Mining and the Environment, CD-ROM, 1121.

Pruess, K., 1991. TOUGH2 – A General Purpose Numerical Simulator for Multiphase Fluid and Heat Transfer. Lawrence Berkeley Laboratory. LBL-29400, 102 pp.

Ptacek, C.J., Blowes, D.W., 2003. Geochemistry of concentrated waters (Chapter 12). In: Jambor, J.L., Blowes, D.W., Ritchie, A.I.M. (Eds.), Environmental Aspects of Mine Wastes, Short Course, vol. 31. Mineralogical Association of Canada, pp. 239–252.

Ritchie, A.I.M., 1994a. The waste rock environment (Chapter 5). In: Jambor, J.L., Blowes, D.W. (Eds.), Short Course Handbook on Environmental Geochemistry of Sulfide Mine Wastes. Mineralogical Association of Canada, Waterloo, Ontario, pp. 133–161.

Ritchie, A.I.M., 1994b. Sulfide oxidation mechanisms: controls and rates of oxygen transport (Chapter 8). In: Jambor, J.L., Blowes, D.W. (Eds.), Short Course Handbook on Environmental Geochemistry of Sulfide Mine Wastes. Mineralogical Association of Canada, Waterloo, Ontario.

Ritchie, A.I.M., 2003. Oxidation and gas transport in piles of sulfidic material (Chapter 4). In: Jambor, J.L., Blowes, D.W., Ritchie, A.I.M. (Eds.), Environmental Aspects of Mine Wastes, Short Course, vol. 31. Mineralogical Association of Canada, pp. 73–94.

Romano, C.G., Mayer, K.U., Jones, D.R., Ellerbroek, D.A., Blowes, D.W., 2003. Effectiveness of various cover scenarios on the rate of sulphide oxidation of mine tailings. J. Hydrol. 271, 171–187.

Schneider, P., Osenbrueck, K., Neitzel, P.L., Nindel, K., 2002. In-situ mitigation of effluents from acid waste rock dumps using reactive surface barriers – a feasibility study. Mine Water Environ. 21, 36–44.

Simunek, J., Sejna, M., van Genuchten, Th.M., 1999. The HYDRUS-2D software package for simulating the two-dimensional movements of water, heat, and multiple solutes in variably-saturated media, Version 2.0. U.S. Salinity Laboratory, Riverside, CA.

Smith, L., Beckie, R., 2003. Hydrologic and geochemical transport processes in mine waste rock (Chapter 3). In: Jambor, J.L., Blowes, D.W., Ritchie, A.I.M. (Eds.), Environmental Aspects of Mine Wastes, Short Course, vol. 31. Mineralogical Association of Canada, pp. 51–72.

Smith, L., Lòpez, D.L., Beckie, R., Dawson, R., Price, W., 1995. Hydrogeology of waste rock dumps. Final Report to Natural Resources Canada, Contract 23440-4-1317/01-SQ, MEND Report PA-1Natural Resources Canada.

Sracek, O., Choquette, M., Gelinas, P., Lefebvre, R., Nicholson, R.V., 2004. Geochemical characterization of acid mine drainage from a waste rock pile, Mine Doyon, Quebec, Canada. J. Contam. Hydrol. 69, 45–71.

Steefel, C.I., MacQuarrie, K.T.B., 1996. Approaches to modeling of reactive transport in porous media. In: Lichtner, P., Steefel, C., Oelkers, E. (Eds.), Reviews in Mineralogy, vol. 34. Mineralogical Society of America, pp. 83–129.

Stumm, W., Morgan, J.J., 1981. Aquatic Chemistry, 2nd ed. John Wiley Inc., New York. 780 pp.

Tran, A.B., Fines, P., Miller, S., Williams, D., Wilson, W., 2003. Hydrologic and geochemical characterization of two full-scale waste rock piles. Geotech. News, 36–42 (Sept. 03).

Valocchi, A., Malmstead, M., 1992. Accuracy of operator splitting for advection–dispersion problems. Water Resour. Res. 28 (5), 1471–1476.

van Genuchten, M.Th., 1980. A closed-form equation for predicting the hydraulic conductivity of unsaturated soils. Soil Sci. Soc. Am. J. 44, 892–898.

Walter, A.L., Frind, E.O., Blowes, D.W., Ptacek, C.J., Molson, J.W., 1994a. Modeling of multicomponent reactive transport in groundwater: 1. Model development and evaluation. Water Resour. Res. 30 (11), 3137–3148.

Walter, A.L., Frind, E.O., Blowes, D.W., Ptacek, C.J., Molson, J.W., 1994b. Modeling of multicomponent reactive transport in groundwater: 2. Metal mobility in aquifers impacted by acid mine tailings discharge. Water Resour. Res. 30 (11), 3149–3158.

Wilson, W., Plewes, H.D., Williams, D., Robertson, J., 2003. Concepts for co-mixing of tailings and waste rock. In: Farrell, T., Taylor, G. (Eds.), Sixth International Conference on Acid Rock Drainage (ICARD). Australasian Institute of Mining and Metallurgy, Cairns, Australia, Publication Series 3/2003, pp. 437–443.

Wunderly, M.D., Blowes, D.W., Frind, E.O., Ptacek, C.J., 1996. Sulfide mineral oxidation and subsequent reactive transport of oxidation products in mine tailings impoundments: a numerical model. Water Resour. Res. 32 (10), 3173–3187.